Available online at www.sciencedirect.com
SCIENCE DIRECT®
Physics Letters B 580 (2004) 37–49
PHYSICS LETTERS B
www.elsevier.com/locate/physletb

Search for scalar leptons and scalar quarks at LEP

L3 Collaboration

P. Achard [t], O. Adriani [q], M. Aguilar-Benitez [x], J. Alcaraz [x], G. Alemanni [v], J. Allaby [r], A. Aloisio [ab], M.G. Alviggi [ab], H. Anderhub [at], V.P. Andreev [f,ag], F. Anselmo [h], A. Arefiev [aa], T. Azemoon [c], T. Aziz [i], P. Bagnaia [al], A. Bajo [x], G. Baksay [y], L. Baksay [y], S.V. Baldew [b], S. Banerjee [i], Sw. Banerjee [d], A. Barczyk [at,ar], R. Barillère [r], P. Bartalini [v], M. Basile [h], N. Batalova [aq], R. Battiston [af], A. Bay [v], F. Becattini [q], U. Becker [m], F. Behner [at], L. Bellucci [q], R. Berbeco [c], J. Berdugo [x], P. Berges [m], B. Bertucci [af], B.L. Betev [at], M. Biasini [af], M. Biglietti [ab], A. Biland [at], J.J. Blaising [d], S.C. Blyth [ah], G.J. Bobbink [b], A. Böhm [a], L. Boldizsar [l], B. Borgia [al], S. Bottai [q], D. Bourilkov [at], M. Bourquin [t], S. Braccini [t], J.G. Branson [an], F. Brochu [d], J.D. Burger [m], W.J. Burger [af], X.D. Cai [m], M. Capell [m], G. Cara Romeo [h], G. Carlino [ab], A. Cartacci [q], J. Casaus [x], F. Cavallari [al], N. Cavallo [ai], C. Cecchi [af], M. Cerrada [x], M. Chamizo [t], Y.H. Chang [av], M. Chemarin [w], A. Chen [av], G. Chen [g], G.M. Chen [g], H.F. Chen [u], H.S. Chen [g], G. Chiefari [ab], L. Cifarelli [am], F. Cindolo [h], I. Clare [m], R. Clare [ak], G. Coignet [d], N. Colino [x], S. Costantini [al], B. de la Cruz [x], S. Cucciarelli [af], J.A. van Dalen [ad], R. de Asmundis [ab], P. Déglon [t], J. Debreczeni [l], A. Degré [d], K. Dehmelt [y], K. Deiters [ar], D. della Volpe [ab], E. Delmeire [t], P. Denes [aj], F. DeNotaristefani [al], A. De Salvo [at], M. Diemoz [al], M. Dierckxsens [b], C. Dionisi [al], M. Dittmar [at], A. Doria [ab], M.T. Dova [j,5], D. Duchesneau [d], M. Duda [a], B. Echenard [t], A. Eline [r], A. El Hage [a], H. El Mamouni [w], A. Engler [ah], F.J. Eppling [m], P. Extermann [t], M.A. Falagan [x], S. Falciano [al], A. Favara [ae], J. Fay [w], O. Fedin [ag], M. Felcini [at], T. Ferguson [ah], H. Fesefeldt [a], E. Fiandrini [af], J.H. Field [t], F. Filthaut [ad], P.H. Fisher [m], W. Fisher [aj], I. Fisk [an], G. Forconi [m], K. Freudenreich [at], C. Furetta [z], Yu. Galaktionov [aa,m], S.N. Ganguli [i], P. Garcia-Abia [x], M. Gataullin [ae], S. Gentile [al], S. Giagu [al], Z.F. Gong [u], G. Grenier [w], O. Grimm [at], M.W. Gruenewald [p], M. Guida [am], R. van Gulik [b], V.K. Gupta [aj], A. Gurtu [i], L.J. Gutay [aq], D. Haas [e], D. Hatzifotiadou [h], T. Hebbeker [a], A. Hervé [r], J. Hirschfelder [ah], H. Hofer [at], M. Hohlmann [y], G. Holzner [at], S.R. Hou [av], Y. Hu [ad], B.N. Jin [g], L.W. Jones [c], P. de Jong [b], I. Josa-Mutuberría [x], D. Käfer [a], M. Kaur [n], M.N. Kienzle-Focacci [t], J.K. Kim [ap], J. Kirkby [r], W. Kittel [ad], A. Klimentov [m,aa], A.C. König [ad], M. Kopal [aq], V. Koutsenko [m,aa], M. Kräber [at], R.W. Kraemer [ah], A. Krüger [as], A. Kunin [m], P. Ladron de Guevara [x], I. Laktineh [w], G. Landi [q], M. Lebeau [r], A. Lebedev [m],

doi:10.1016/j.physletb.2003.10.010

P. Lebrun [w], P. Lecomte [at], P. Lecoq [r], P. Le Coultre [at], J.M. Le Goff [r], R. Leiste [as], M. Levtchenko [z], P. Levtchenko [ag], C. Li [u], S. Likhoded [as], C.H. Lin [av], W.T. Lin [av], F.L. Linde [b], L. Lista [ab], Z.A. Liu [g], W. Lohmann [as], E. Longo [al], Y.S. Lu [g], C. Luci [al], L. Luminari [al], W. Lustermann [at], W.G. Ma [u], L. Malgeri [t], A. Malinin [aa], C. Maña [x], J. Mans [aj], J.P. Martin [w], F. Marzano [al], K. Mazumdar [i], R.R. McNeil [f], S. Mele [r,ab], L. Merola [ab], M. Meschini [q], W.J. Metzger [ad], A. Mihul [k], H. Milcent [r], G. Mirabelli [al], J. Mnich [a], G.B. Mohanty [i], G.S. Muanza [w], A.J.M. Muijs [b], B. Musicar [an], M. Musy [al], S. Nagy [o], S. Natale [t], M. Napolitano [ab], F. Nessi-Tedaldi [at], H. Newman [ae], A. Nisati [al], T. Novak [ad], H. Nowak [as], R. Ofierzynski [at], G. Organtini [al], I. Pal [aq], C. Palomares [x], P. Paolucci [ab], R. Paramatti [al], G. Passaleva [q], S. Patricelli [ab], T. Paul [j], M. Pauluzzi [af], C. Paus [m], F. Pauss [at], M. Pedace [al], S. Pensotti [z], D. Perret-Gallix [d], B. Petersen [ad], D. Piccolo [ab], F. Pierella [h], M. Pioppi [af], P.A. Piroué [aj], E. Pistolesi [z], V. Plyaskin [aa], M. Pohl [t], V. Pojidaev [q], J. Pothier [r], D. Prokofiev [ag], J. Quartieri [am], G. Rahal-Callot [at], M.A. Rahaman [i], P. Raics [o], N. Raja [i], R. Ramelli [at], P.G. Rancoita [z], R. Ranieri [q], A. Raspereza [as], P. Razis [ac], D. Ren [at], M. Rescigno [al], S. Reucroft [j], S. Riemann [as], K. Riles [c], B.P. Roe [c], L. Romero [x], A. Rosca [as], S. Rosier-Lees [d], S. Roth [a], C. Rosenbleck [a], J.A. Rubio [r], G. Ruggiero [q], H. Rykaczewski [at], A. Sakharov [at], S. Saremi [f], S. Sarkar [al], J. Salicio [r], E. Sanchez [x], C. Schäfer [r], V. Schegelsky [ag], H. Schopper [au], D.J. Schotanus [ad], C. Sciacca [ab], L. Servoli [af], S. Shevchenko [ae], N. Shivarov [ao], V. Shoutko [m], E. Shumilov [aa], A. Shvorob [ae], D. Son [ap], C. Souga [w], P. Spillantini [q], M. Steuer [m], D.P. Stickland [aj], B. Stoyanov [ao], A. Straessner [t], K. Sudhakar [i], G. Sultanov [ao], L.Z. Sun [u], S. Sushkov [a], H. Suter [at], J.D. Swain [j], Z. Szillasi [y,3], X.W. Tang [g], P. Tarjan [o], L. Tauscher [e], L. Taylor [j], B. Tellili [w], D. Teyssier [w], C. Timmermans [ad], Samuel C.C. Ting [m], S.M. Ting [m], S.C. Tonwar [i], J. Tóth [l], C. Tully [aj], K.L. Tung [g], J. Ulbricht [at], E. Valente [al], R.T. Van de Walle [ad], R. Vasquez [aq], V. Veszpremi [y], G. Vesztergombi [l], I. Vetlitsky [aa], D. Vicinanza [am], G. Viertel [at], S. Villa [ak], M. Vivargent [d], S. Vlachos [e], I. Vodopianov [y], H. Vogel [ah], H. Vogt [as], I. Vorobiev [ah,aa], A.A. Vorobyov [ag], M. Wadhwa [e], Q. Wang [ad], X.L. Wang [u], Z.M. Wang [u], M. Weber [a], P. Wienemann [a], H. Wilkens [ad], S. Wynhoff [aj], L. Xia [ae], Z.Z. Xu [u], J. Yamamoto [c], B.Z. Yang [u], C.G. Yang [g], H.J. Yang [c], M. Yang [g], S.C. Yeh [aw], An. Zalite [ag], Yu. Zalite [ag], Z.P. Zhang [u], J. Zhao [u], G.Y. Zhu [g], R.Y. Zhu [ae], H.L. Zhuang [g], A. Zichichi [h,r,s], B. Zimmermann [at], M. Zöller [a]

[a] *III. Physikalisches Institut, RWTH, D-52056 Aachen, Germany* [l]
[b] *National Institute for High Energy Physics, NIKHEF, and University of Amsterdam, NL-1009 DB Amsterdam, The Netherlands*
[c] *University of Michigan, Ann Arbor, MI 48109, USA*
[d] *Laboratoire d'Annecy-le-Vieux de Physique des Particules, LAPP, IN2P3-CNRS, BP 110, F-74941 Annecy-le-Vieux cedex, France*
[e] *Institute of Physics, University of Basel, CH-4056 Basel, Switzerland*
[f] *Louisiana State University, Baton Rouge, LA 70803, USA*
[g] *Institute of High Energy Physics, IHEP, 100039 Beijing, China* [6]
[h] *University of Bologna and INFN-Sezione di Bologna, I-40126 Bologna, Italy*

[i] Tata Institute of Fundamental Research, Mumbai (Bombay) 400 005, India
[j] Northeastern University, Boston, MA 02115, USA
[k] Institute of Atomic Physics and University of Bucharest, R-76900 Bucharest, Romania
[l] Central Research Institute for Physics of the Hungarian Academy of Sciences, H-1525 Budapest 114, Hungary [2]
[m] Massachusetts Institute of Technology, Cambridge, MA 02139, USA
[n] Panjab University, Chandigarh 160 014, India
[o] KLTE-ATOMKI, H-4010 Debrecen, Hungary [3]
[p] Department of Experimental Physics, University College Dublin, Belfield, Dublin 4, Ireland
[q] INFN-Sezione di Firenze and University of Florence, I-50125 Florence, Italy
[r] European Laboratory for Particle Physics, CERN, CH-1211 Geneva 23, Switzerland
[s] World Laboratory, FBLJA Project, CH-1211 Geneva 23, Switzerland
[t] University of Geneva, CH-1211 Geneva 4, Switzerland
[u] Chinese University of Science and Technology, USTC, Hefei, Anhui 230 029, China [6]
[v] University of Lausanne, CH-1015 Lausanne, Switzerland
[w] Institut de Physique Nucléaire de Lyon, IN2P3-CNRS, Université Claude Bernard, F-69622 Villeurbanne, France
[x] Centro de Investigaciones Energéticas, Medioambientales y Tecnológicas, CIEMAT, E-28040 Madrid, Spain [4]
[y] Florida Institute of Technology, Melbourne, FL 32901, USA
[z] INFN-Sezione di Milano, I-20133 Milan, Italy
[aa] Institute of Theoretical and Experimental Physics, ITEP, Moscow, Russia
[ab] INFN-Sezione di Napoli and University of Naples, I-80125 Naples, Italy
[ac] Department of Physics, University of Cyprus, Nicosia, Cyprus
[ad] University of Nijmegen and NIKHEF, NL-6525 ED Nijmegen, The Netherlands
[ae] California Institute of Technology, Pasadena, CA 91125, USA
[af] INFN-Sezione di Perugia and Università Degli Studi di Perugia, I-06100 Perugia, Italy
[ag] Nuclear Physics Institute, St. Petersburg, Russia
[ah] Carnegie Mellon University, Pittsburgh, PA 15213, USA
[ai] INFN-Sezione di Napoli and University of Potenza, I-85100 Potenza, Italy
[aj] Princeton University, Princeton, NJ 08544, USA
[ak] University of Californa, Riverside, CA 92521, USA
[al] INFN-Sezione di Roma and University of Rome, "La Sapienza", I-00185 Rome, Italy
[am] University and INFN, Salerno, I-84100 Salerno, Italy
[an] University of California, San Diego, CA 92093, USA
[ao] Bulgarian Academy of Sciences, Central Laboratory of Mechatronics and Instrumentation, BU-1113 Sofia, Bulgaria
[ap] The Center for High Energy Physics, Kyungpook National University, 702-701 Taegu, Republic of Korea
[aq] Purdue University, West Lafayette, IN 47907, USA
[ar] Paul Scherrer Institut, PSI, CH-5232 Villigen, Switzerland
[as] DESY, D-15738 Zeuthen, Germany
[at] Eidgenössische Technische Hochschule, ETH Zürich, CH-8093 Zürich, Switzerland
[au] University of Hamburg, D-22761 Hamburg, Germany
[av] National Central University, Chung-Li, Taiwan, ROC
[aw] Department of Physics, National Tsing Hua University, Taiwan, ROC

Received 31 July 2003; received in revised form 18 September 2003; accepted 4 October 2003

Editor: L. Rolandi

Abstract

Scalar partners of quarks and leptons, predicted in supersymmetric models, are searched for in e^+e^- collisions at centre-of-mass energies between 192 and 209 GeV at LEP. No evidence for any such particle is found in a data sample of 450 pb^{-1}. Upper limits on their production cross sections are set and lower limits on their masses are derived in the framework of the Minimal Supersymmetric Standard Model.

1. Introduction

The minimal supersymmetric extension of the Standard Model (MSSM) [1,2] postulates a scalar partner, $\tilde{f}_{L,R}$, for each weak eigenstate of Standard Model (SM) fermions $f_{L,R}$. Generally, the left, $\tilde{f}_L$, and right, $\tilde{f}_R$, eigenstates mix to form mass eigenstates. This mixing is an unitary transformation of the $\tilde{f}_R$ and $\tilde{f}_L$ states, parameterised by a mixing angle, θ_{LR}. Since the off-diagonal elements of the sfermion mass matrix are proportional to the SM partner mass, the mixing is expected to be relevant only for scalar fermions of the third family: the scalar top, $\tilde{t}_{L,R}$, the scalar bottom, $\tilde{b}_{L,R}$, and the scalar tau, $\tilde{\tau}_{L,R}$. The lightest scalar quarks are denoted as $\tilde{t}_1$ and $\tilde{b}_1$.

The R-parity is a quantum number which distinguishes SM particles from supersymmetric particles. If R-parity is conserved, supersymmetric particles are pair-produced and the lightest supersymmetric particle, assumed hereafter to be the lightest neutralino, $\tilde{\chi}_1^0$, is stable. In addition, the $\tilde{\chi}_1^0$ is weakly-interacting and hence escapes detection. R-parity conservation is assumed in the following, which implies that the decay chain of pair-produced supersymmetric particles always contains, besides the relevant SM particles, at least two invisible neutralinos. The typical signature of the production of scalar leptons and scalar quarks is the presence of leptons or jets in events with missing energy and momentum. The difference between the masses of the scalar fermion and the $\tilde{\chi}_1^0$, ΔM, determines the kinematic of the event.

The pair-production of scalar fermions in e^+e^- interactions proceeds through the s-channel γ or Z exchange. For scalar electrons, the production cross section is typically enhanced by the t-channel exchange of a neutralino.

At LEP energies, all scalar fermions, but the scalar top, decay into their SM partners mainly via $\tilde{f} \to \tilde{\chi}_1^0 f$. Cascade decays, such as $\tilde{f} \to \tilde{\chi}_2^0 f \to \tilde{\chi}_1^0 Z^* f$ are also possible and may dominate in some regions of the MSSM parameter space. According to the values of the scalar top mass and couplings, four channels can become dominant among the possible scalar top decays: $\tilde{t}_1 \to c\tilde{\chi}_1^0$, $b\nu_\ell\tilde{\ell}$, $b\ell\tilde{\nu}_\ell$ and $b\tilde{\chi}_1^+$. The additional decay into $b\tilde{\chi}_1^0 f\bar{f}'$ which can originate six-fermion final states is not considered [3]. This topology is indirectly covered by searches in the framework of R-parity violation, which revealed no excess [4]. In the following, for the $\tilde{t} \to \tilde{\nu} b\ell$ decay, scalar neutrinos are assumed to be lighter than charged scalar leptons. For this decay, ΔM refers to the mass difference between the scalar top and scalar neutrino masses.

The supersymmetric partners of the right-handed leptons, $\tilde{\ell}_R$, are generally expected to be lighter than their left-handed counterparts and are considered in the following. If the mass difference between the right-handed scalar electron and the lightest neutralino is very small the search for $e^+e^- \to \tilde{e}_R\tilde{e}_R$ has little sensitivity. The $e^+e^- \to \tilde{e}_R\tilde{e}_L$ process is then considered. The left-handed scalar electron, too heavy to be produced in pairs, decays into an energetic electron, while the electron from the right-handed scalar electron decay remains often invisible, leading to a 'single electron' topology.

Scalar leptons and scalar quarks are searched for at centre-of-mass energies, $\sqrt{s}$, up to 209 GeV. The present study supersedes previous L3 limits on scalar lepton [5] and scalar quark production [6] obtained at lower $\sqrt{s}$. Searches for scalar fermions were also reported by other experiments at LEP [7] and at the TEVATRON [8]. Table 1 summarises the investigated

Table 1
Summary of the investigated processes, decay modes and studied topologies

Process	Decay mode	Topology
$e^+e^- \to \tilde{\ell}_R\bar{\tilde{\ell}}_R$	$\tilde{\ell}_R \to \tilde{\chi}_1^0\ell$	Acoplanar leptons
$e^+e^- \to \tilde{e}_R\tilde{e}_L$	$\tilde{e}_{L,R} \to \tilde{\chi}_1^0 e$	Single electron
$e^+e^- \to \tilde{b}\bar{\tilde{b}}$	$\tilde{b} \to \tilde{\chi}_1^0 b$	Acoplanar b-jets
$e^+e^- \to \tilde{t}\bar{\tilde{t}}$	$\tilde{t} \to \tilde{\chi}_1^0 c$	Acoplanar jets
$e^+e^- \to \tilde{t}\bar{\tilde{t}}$	$\tilde{t} \to \tilde{\nu} b\ell$	Acoplanar jets and leptons
$e^+e^- \to \tilde{q}\bar{\tilde{q}}$	$\tilde{q} \to \tilde{\chi}_1^0 q$	Acoplanar jets

[1] Supported by the German Bundesministerium für Bildung, Wissenschaft, Forschung und Technologie.
[2] Supported by the Hungarian OTKA fund under Contract Nos. T019181, F023259 and T037350.
[3] Also supported by the Hungarian OTKA fund under Contract No. T026178.
[4] Also supported by the Comisión Interministerial de Ciencia y Tecnología.
[5] Also supported by CONICET and Universidad Nacional de La Plata, CC 67, 1900 La Plata, Argentina.
[6] Supported by the National Natural Science Foundation of China.

processes and decay modes together with the studied topology.

2. Data samples and Monte Carlo simulation

The data used in the present analysis were collected with the L3 detector [9] at LEP and correspond to an integrated luminosity of 450.5 pb^{-1} at $\sqrt{s} = 192$–209 GeV. Two average centre-of-mass energies are considered in the following: 196 and 205 GeV, with corresponding integrated luminosities of 233.2 and 217.3 pb^{-1}.

SM processes are simulated with the following Monte Carlo (MC) generators: PYTHIA [10] for $e^+e^- \to q\bar{q}(\gamma)$, $e^+e^- \to Ze^+e^-$ and $e^+e^- \to ZZ$, EXCALIBUR [11] for $e^+e^- \to W^{\pm}e^{\mp}\nu$, KORALZ [12] for $e^+e^- \to \mu^+\mu^-(\gamma)$ and $e^+e^- \to \tau^+\tau^-(\gamma)$, BHWIDE [13] for $e^+e^- \to e^+e^-(\gamma)$ and KORALW [14] for $e^+e^- \to W^+W^-$. Two-photon interaction processes are simulated using DIAG36 [15] for $e^+e^- \to e^+e^-\ell^+\ell^-$ and PHOJET [16] for $e^+e^- \to e^+e^-$ hadrons, requiring at least 3 GeV for the invariant mass of the two-photon system. The number of simulated events for each background process is more than 100 times the data statistics, except for two-photon processes for which the MC statistics amounts to about 7 times that of the data.

Signal events for scalar leptons are generated with the SUSYGEN [17] MC program, for scalar lepton masses, $M_{\tilde{\ell}}$, ranging from 45 GeV up to the kinematic limit, and for values of ΔM varying between 3 GeV and $M_{\tilde{\ell}} - 1$ GeV. For scalar quarks, a generator [18] based on PYTHIA is used. Scalar quark masses vary

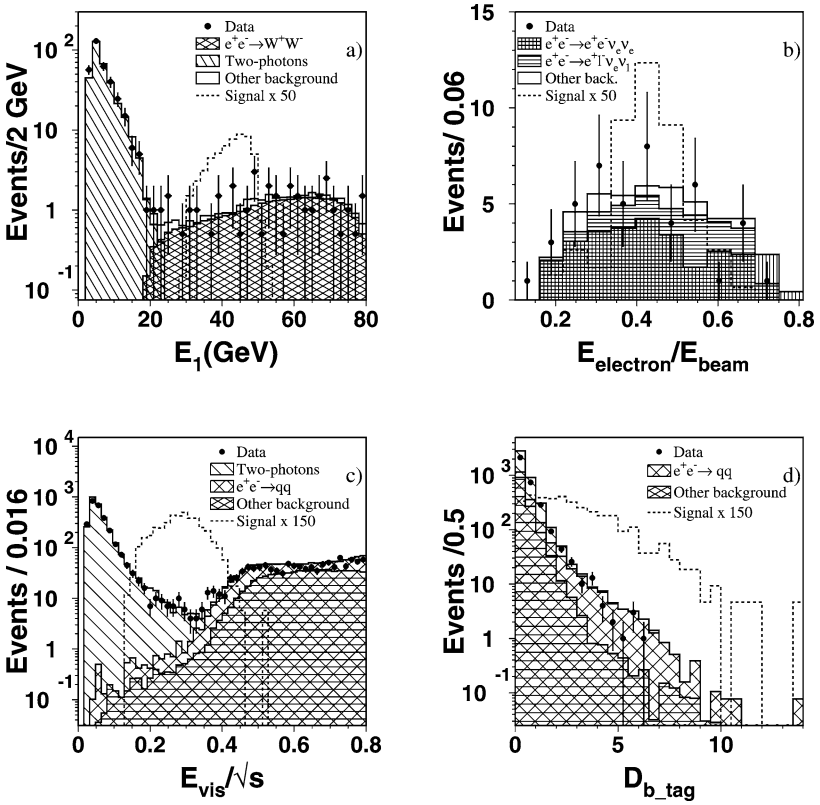

Fig. 1. Distributions in data and MC of the energy of the most energetic lepton of the (a) scalar lepton searches and (b) single electron analysis. (c) Visible energy and (d) b-tag variable for the scalar quark analysis. Signal events are scaled by the factors indicated in the figures and correspond to (a) $M_{\tilde{\ell}_R} = 90$ GeV and $M_{\tilde{\chi}_1^0} = 40$ GeV, (b) $M_{\tilde{e}_L} = 110$ GeV and $M_{\tilde{\chi}_1^0} = 50$ GeV, (c) and (d) $\tilde{t}_1 \to c\tilde{\chi}_1^0$ decay for $M_{\tilde{t}_R} = 90$ GeV, $M_{\tilde{\chi}_1^0} = 60$ GeV.

Table 2
Results of the scalar lepton analysis: number of observed events, N_D, SM background expectations, N_{SM}, and efficiencies, ε, at $\sqrt{s} = 205$ GeV for the scalar electron, muon and tau selections at low ($Z < 10$ GeV), medium (10 GeV $< Z <$ 30 GeV) and high ΔM ($Z > 30$ GeV) for different values of the scalar lepton masses

	$\tilde{e}$ $M_{\tilde{e}} = 94$ GeV			$\tilde{\mu}$ $M_{\tilde{\mu}} = 90$ GeV			$\tilde{\tau}$ $M_{\tilde{\tau}} = 80$ GeV		
	N_D	N_{SM}	ε (%)	N_D	N_{SM}	ε (%)	N_D	N_{SM}	ε (%)
Low ΔM	79	84	10	151	138	29	317	270	3
Medium ΔM	19	25	45	46	47	52	146	124	29
High ΔM	50	53	35	108	105	57	122	123	29

Table 3
Results of the scalar quark analysis: number of observed events, N_D, SM background expectations, N_{SM}, and efficiencies, ε, for a 90 GeV scalar quark at very low (5–10 GeV), low (10–20 GeV), medium (20–40 GeV) and high ΔM ($\geqslant 40$ GeV) at $\sqrt{s} = 205$ GeV

	$\tilde{t}_1 \to c\tilde{\chi}_1^0$			$\tilde{t}_1 \to b\ell\tilde{\nu}$			$\tilde{t}_1 \to b\tau\tilde{\nu}$			$\tilde{b}_1 \to b\tilde{\chi}_1^0$		
	N_D	N_{SM}	ε (%)	N_D	N_{SM}	ε (%)	N_D	N_{SM}	ε (%)	N_D	N_{SM}	ε (%)
Very low ΔM	23	21.6	18	2	2.2	5	1	1.3	6	1	3.8	13
Low ΔM	1	3.1	22	0	0.4	14	0	1.6	16	1	2.3	22
Medium ΔM	4	1.3	36	2	1.4	18	2	0.5	23	2	1.5	42
High ΔM	1	1.9	15	1	0.7	13	3	0.7	25	2	1.6	21

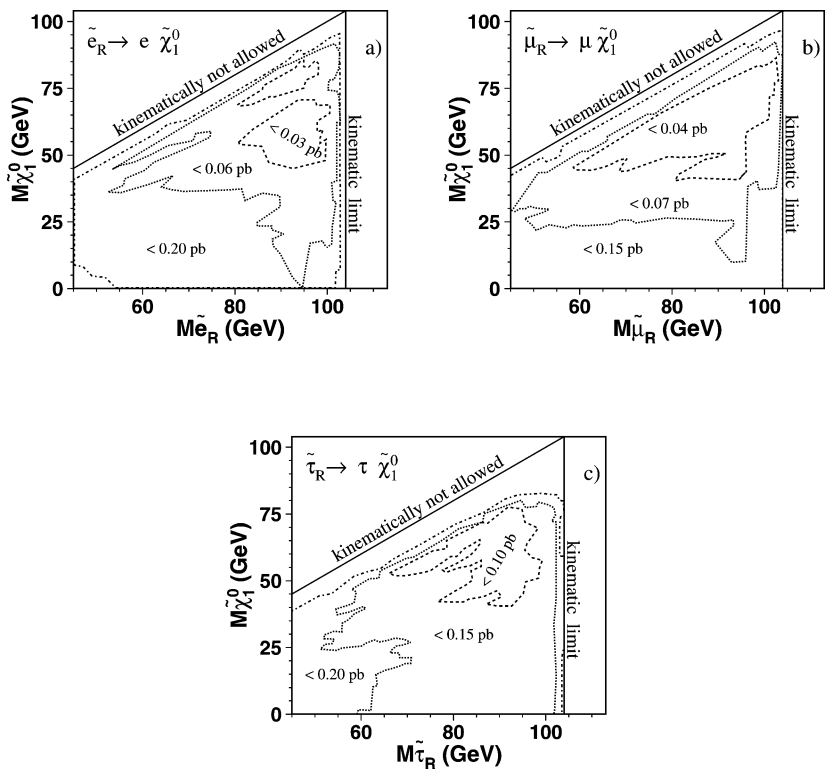

Fig. 2. Model independent upper limits on the $e^+e^- \to \tilde{\ell}_R\bar{\tilde{\ell}}_R$ cross section in the $M_{\tilde{\chi}_1^0}$–$M_{\tilde{\ell}}$ plane, for (a) scalar electrons, (b) scalar muons and (c) scalar taus.

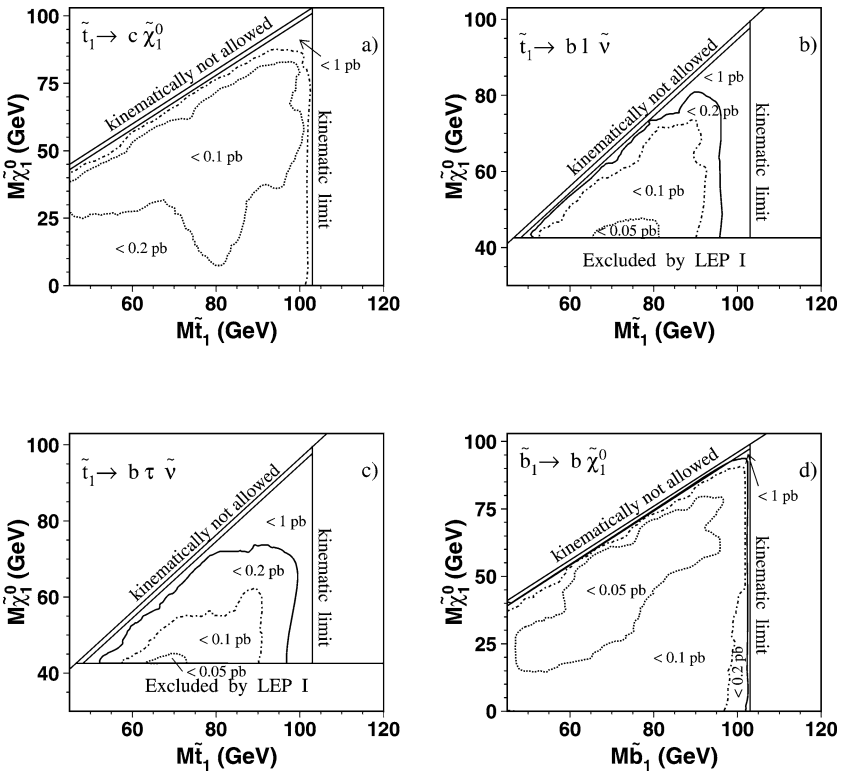

Fig. 3. Model independent upper limits on the (a), (b) and (c) $e^+e^- \to \tilde{t}_1\bar{\tilde{t}}_1$ and (d) $e^+e^- \to \tilde{b}_1\bar{\tilde{b}}_1$ production cross sections multiplied by the branching ratio of the decay mode: (a) $\tilde{t}_1 \to c\tilde{\chi}_1^0$, (b) $\tilde{t}_1 \to b\ell\tilde{\nu}$, (c) $\tilde{t}_1 \to b\tau\tilde{\nu}$ and (d) $\tilde{b}_1 \to b\tilde{\chi}_1^0$.

Table 4
Summary of the number of observed data events, N_D, and SM background expectations, N_{SM}, for all the studied topologies

Process	Decay mode	N_D	N_{SM}
$e^+e^- \to \tilde{e}\bar{\tilde{e}}$	$\tilde{e} \to \tilde{\chi}_1^0 e$	143	153
$e^+e^- \to \tilde{\mu}\bar{\tilde{\mu}}$	$\tilde{\mu} \to \tilde{\chi}_1^0 \mu$	269	253
$e^+e^- \to \tilde{\tau}\bar{\tilde{\tau}}$	$\tilde{\tau} \to \tilde{\chi}_1^0 \tau$	410	381
$e^+e^- \to \tilde{e}_R\tilde{e}_L$	$\tilde{e}_{L,R} \to \tilde{\chi}_1^0 e$	45	44.6
$e^+e^- \to \tilde{b}\bar{\tilde{b}}$	$\tilde{b} \to \tilde{\chi}_1^0 b$	6	7.7
$e^+e^- \to \tilde{t}\bar{\tilde{t}}$	$\tilde{t} \to \tilde{\chi}_1^0 c$	29	26.5
$e^+e^- \to \tilde{t}\bar{\tilde{t}}$	$\tilde{t} \to \tilde{\nu} b\ell$	4	4.0
$e^+e^- \to \tilde{t}\bar{\tilde{t}}$	$\tilde{t} \to \tilde{\nu} b\tau$	5	3.9

from 45 GeV up to the kinematical limit and $M_{\tilde{\chi}_1^0}$ varies from 1 GeV to $M_{\tilde{t}_1} - 3$ GeV and to $M_{\tilde{b}_1} - 7$ GeV, for scalar top and bottom, respectively. The $\tilde{t}_1 \to b\ell\tilde{\nu}$ and $\tilde{t}_1 \to b\tau\tilde{\nu}$ channels are generated with $\tilde{\nu}$ mass ranging from the 43 GeV limit [19] up to $M_{\tilde{t}_1} -$ 8 GeV. In total, about 180 samples are generated, each with at least 1000 events.

The response of the L3 detector is simulated using the GEANT package [20]. It takes into account effects of energy loss, multiple scattering and showering in the detector materials and in the beam pipe. Hadronic interactions are simulated with the GHEISHA program [21]. Time-dependent detector inefficiencies are monitored during data taking and reproduced in the simulation.

3. Event selection

3.1. Analysis procedure

Besides the common signature of missing momentum in the direction transverse to the beam axis, signals from supersymmetric particles are further speci-

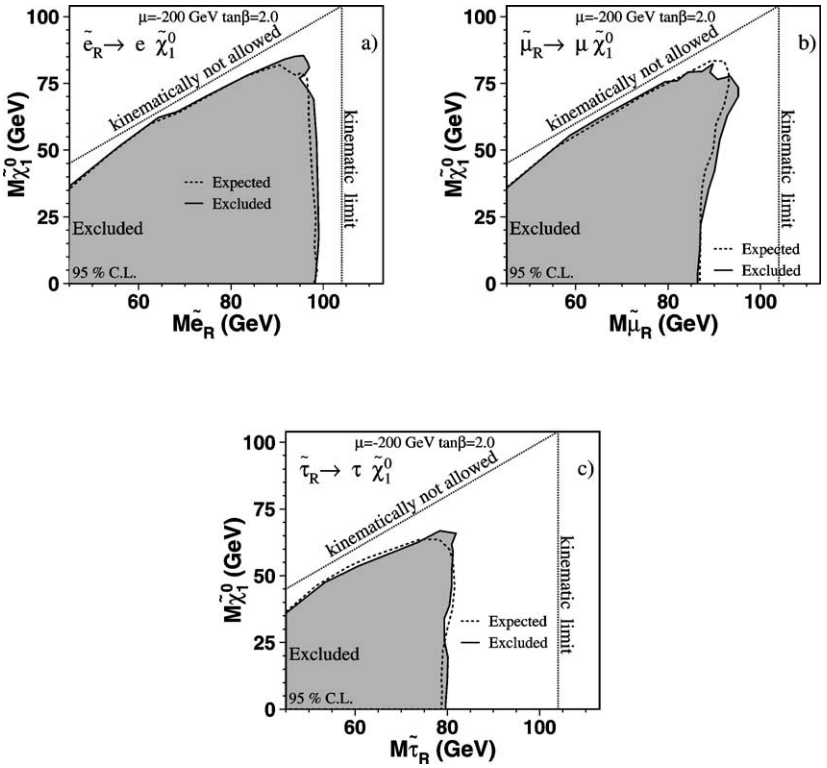

Fig. 4. Regions of the plane $M_{\tilde{\chi}_1^0}$–$M_{\tilde{\ell}_R}$ excluded in the MSSM for (a) scalar electrons, (b) scalar muons and (c) scalar taus.

fied according to the number of leptons or the multiplicity of hadronic jets in the final state.

Signatures of scalar leptons are simple and the final states mostly contain just two acoplanar leptons of the same generation. To account for the three lepton flavours, three different selections are performed. For scalar electrons and muons a pair of electrons or muons is required in the event, respectively, while scalar taus are selected as low-multiplicity events with electrons or muons or with narrow jets. Events from the $\tilde{t}_1 \rightarrow c\tilde{\chi}_1^0$ and $\tilde{b}_1 \rightarrow b\tilde{\chi}_1^0$ processes contain two high-multiplicity acoplanar jets originated by c or b quarks. In addition, two charged leptons are present when both scalar top quarks decay via $\tilde{t}_1 \rightarrow b\ell\tilde{\nu}$.

An optimization procedure is devised [5] which maximizes signal efficiency and background rejection by varying simultaneously all cuts for a given process. The signal topology depends on ΔM and therefore the optimization is repeated for different values of ΔM. Details of the selections performed for each topology are given in the following.

3.2. Acoplanar leptons

Scalar leptons are searched for in events with two isolated leptons of the same flavour. The lepton identification and isolation criteria follow those used at lower $\sqrt{s}$ [22]. An electron is isolated if the calorimetric energy deposition in a 10° cone around its direction is less than 2 GeV. Muon isolation requires an energy below 2 GeV in the cone between 5° and 10° around the muon direction. A tau is isolated if the energy deposition in the cone between 10° and 20° around its direction is less than 2 GeV and less than 50% of the tau energy. Furthermore, the energy deposition in a cone between 20° and 30° must be less than 60% of the tau energy.

The large background from two-photon interactions is rejected with cuts on the lepton transverse momentum, the visible mass, $M_{\rm vis}$, the transverse missing momentum, $P_T^{\rm miss}$, the energy deposited at low polar angle, E_{30}, and the sine of the polar angle of the missing momentum, $\sin\theta_{\rm miss}$. Acoplanarity and acollinear-

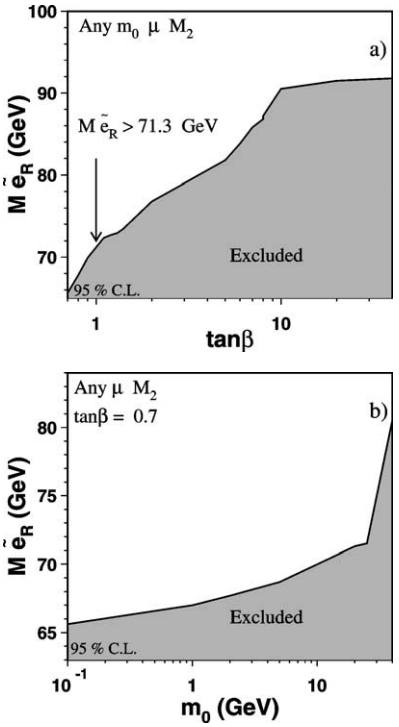

Fig. 5. Absolute $\tilde{e}_R$ mass limit as a function of (a) $\tan\beta$ and (b) m_0.

ity cuts together with upper bounds on the visible energy, E_{vis}, reduce the background from W boson and fermion pair-production. After these cuts, the distributions of selection variables for data and Monte Carlo are in good agreement, as shown in Fig. 1(a) for the energy of the most energetic lepton, E_1.

The final selections are optimised for each scalar lepton flavour, using a set of parameterized cuts (E_{vis}, P_T^{miss}, M_{vis}, E_1) together with fixed cuts (acoplanarity, acollinearity and $\sin\theta_{\text{miss}}$). The parameterised cuts depend on $Z = (\Delta M/M_{\tilde{\ell}}) \times E_{\text{beam}}$, to reflect the dependence of the final state topologies on ΔM and $M_{\tilde{\ell}}$. E_{beam} is the beam energy. The variables used for each selection are described in Ref. [5].

The selection efficiencies for scalar lepton pair-production, the number of candidates in data and the SM expectations are given in Table 2 for three ΔM regions.

3.3. Single electron

The single-electron analysis requires one or two identified electrons. Cuts on E_{vis} and $\sin\theta_{\text{miss}}$ are applied in order to reject background from two-photon interactions. At least one electron with energy greater than 5 GeV is required. The electron energy has to be less than 65 GeV to reject photon conversion from the $e^+e^- \to \nu\bar{\nu}\gamma$ process when the two tracks are not resolved. If two electrons are selected, their acoplanarity must be between 10° and 160° and the energy of the second electron must be less than 5 GeV to suppress background from W pair-production. To remove events with additional activity in the detector, the difference between the total energy and the energy of the most energetic electron must be less than 5 GeV. In addition, a cut $P_T^{\text{miss}} > 15$ GeV is applied. If no second electron of at least 100 MeV is detected, this cut is released to $P_T^{\text{miss}} > 10$ GeV. Fig. 1(b) compares data and MC for the energy of the most energetic electron, the remaining background originates from four-fermion final states. Signal efficiencies vary from 3% at $\Delta M = M_{\tilde{e}_L} - M_{\tilde{\chi}_1^0} = 5$ GeV up to 60% for $\Delta M = 60$ GeV.

3.4. Acoplanar jets

The search for scalar quarks decaying into quarks and neutralino is based on events with two high-multiplicity acoplanar jets. The DURHAM algorithm [23] is used for the clustering of hadronic jets. A common preselection is applied [6] which is based on: E_{vis}, the calorimetric cluster multiplicity, P_T^{miss}, E_{30} and $\sin\theta_{\text{miss}}$. After this preselection, the data agree well with the SM expectations, as depicted in Fig. 1(c) and (d).

Four selections are optimised for scalar top quarks and four for scalar bottom quarks. They depend on ΔM and cover the regions 5–10, 10–20, 20–40 GeV and above 40 GeV. Lower cuts on $E_{\text{vis}}/\sqrt{s}$ and $P_T^{\text{miss}}/\sqrt{s}$ separate the signal from the two-photon background, whereas an upper cut on $E_{\text{vis}}/\sqrt{s}$ removes events from four-fermion final states. A cut on $\sin\theta_{\text{miss}}$ also rejects the two-photon background. Cuts on the jet widths and on the absolute value of the projection of the total momentum of the jets onto the direction perpendicular to thrust, computed in the transverse plane, further suppress the two-photon as well as W^+W^- and $q\bar{q}(\gamma)$ backgrounds.

For the scalar bottom selection, b-quark identification in the final state is enforced by an additional cut on the event b-tagging variable [6], $D_{\text{b-tag}}$.

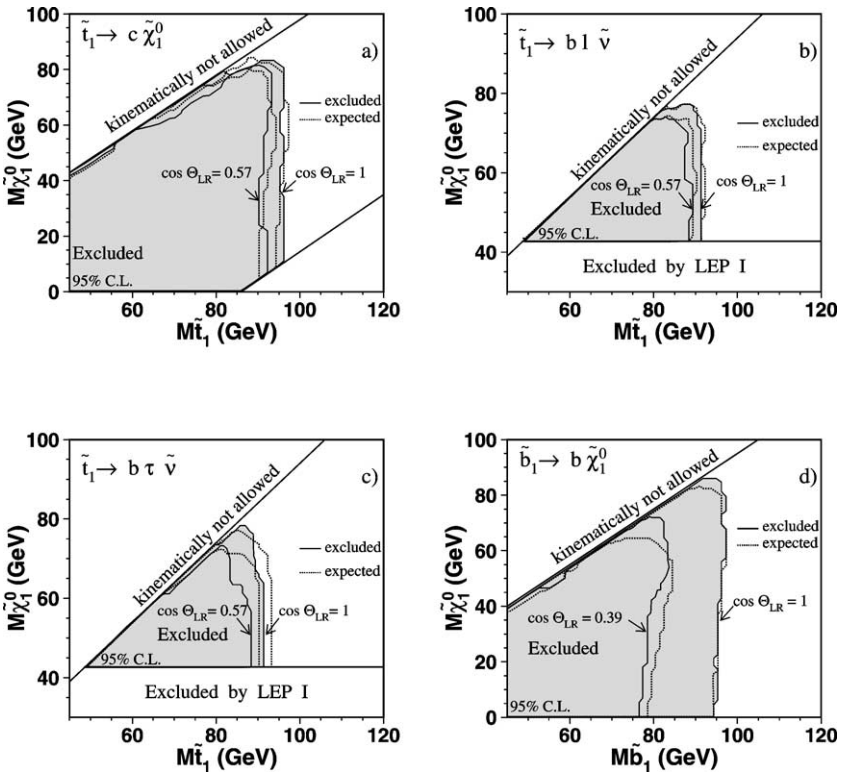

Fig. 6. Regions excluded in the planes (a), (b) and (c) $M_{\tilde{\chi}_1^0}$–$M_{\tilde{t}_1}$ and (d) $M_{\tilde{\chi}_1^0}$–$M_{\tilde{b}_1}$. The MSSM decay modes: (a) $\tilde{t}_1 \to c\tilde{\chi}_1^0$, (b) $\tilde{t}_1 \to b\ell\tilde{\nu}$, (c) $\tilde{t}_1 \to b\tau\tilde{\nu}$ and (d) $\tilde{b}_1 \to b\tilde{\chi}_1^0$ are studied. Different values of the mixing angles are considered.

The expected signal efficiencies at various ΔM values are given in Table 3 together with the observed number of events and the SM background expectations.

3.5. Acoplanar jets and leptons

A selection of events with two acoplanar jets and one or two isolated leptons complements the scalar top searches in presence of the $\tilde{t}_1 \to b\ell\tilde{\nu}$ decay. Large values of the $D_{\text{b-tag}}$ variables are required for the two jets and additional cuts on $E_{\text{vis}}/\sqrt{s}$ reject part of the two-photon and four-fermion events. Lower cuts on the energy of the leptons suppress background from two-photon interactions at low ΔM and the $q\bar{q}(\gamma)$ final state at medium ΔM. At high ΔM, an upper cut on the lepton energy reject four-fermion events. This selection covers the ΔM region above the limit $M_{\tilde{\nu}} > 43$ GeV.

The expected signal efficiencies for scalar top detection are given in Table 3 together with data counts and the SM background expectations, for various ΔM values.

4. Results

4.1. Cross section limits

As discussed above and summarized in Table 4, no excess with respect to the Standard Model expectations is observed in the data. Upper limits on the production cross section are therefore derived combining these results with those obtained at lower $\sqrt{s}$ [5,6]. This combination scales the signal cross sections with $\sqrt{s}$ and the limits refer to $\sqrt{s} = 205$ GeV.

Figs. 2 and 3 show the 95% confidence level (CL) upper bounds on the production cross sections as a function of the scalar fermion masses and of the neu-

tralino mass. The case of right-handed scalar leptons and of the lightest scalar quarks is considered. These limits include [24] the systematics effects discussed below.

4.2. Systematic uncertainties

Systematic uncertainties on the signal efficiency for scalar lepton searches and on all background predictions are dominated by Monte Carlo statistics. They are smaller than 5%. The main systematic uncertainties on the scalar quark signal selection efficiency arise from uncertainties on the production mechanism, hadronisation and decay of the scalar quark [6]. These uncertainties are in the range from 7 to 18% for scalar top, with the highest uncertainty in the very low ΔM region. For scalar bottom, the highest uncertainty is about 10% and is observed in the very low and high ΔM regions.

5. Interpretations in the MSSM

In the MSSM, with grand unification assumptions [25], the masses and couplings of the supersymmetric particles as well as their production cross sections are described [2] in terms of five parameters: $\tan\beta$, the ratio of the vacuum expectation values of the two Higgs doublets, $M_2 \simeq 0.81 \times m_{1/2}$, the gaugino mass parameter, μ, the Higgsino mixing parameter, m_0, the common mass for scalar fermions at the GUT scale and A_0, the trilinear coupling in the scalar fermion sector. We investigate the following MSSM parameter space:

$$1 \leqslant \tan\beta \leqslant 60, \qquad 0 \leqslant M_2 \leqslant 2000\ \text{GeV},$$
$$-2000 \leqslant \mu \leqslant 2000\ \text{GeV}, \qquad 0 \leqslant m_0 \leqslant 500\ \text{GeV},$$
$$-1000 < A_0 < 1000\ \text{GeV}.$$

The limits on the production cross section for scalar leptons and scalar quarks discussed above are translated into exclusion regions in the MSSM parameter space. To derive these limits, we optimise the event selection for each point in the MSSM parameter space by choosing the combination of selections which provides the highest sensitivity for each process. This sensitivity is derived by calculating at each point the production cross sections and the decay branching fractions of scalar leptons and scalar quarks. For the latter, the mixing angle θ_{LR} is also considered. A point of the MSSM parameter space is excluded if any of these calculated cross sections exceeds its corresponding experimental limit. Mass lower limits are derived as the lowest value for the mass of a particle over all points which are not excluded.

5.1. Limits on scalar lepton masses

Fig. 4(a)–(c) shows the exclusion contours in the $M_{\tilde{\chi}_1^0}$–$M_{\tilde{\ell}_{\mathrm{R}}}$ plane obtained by considering only the reaction $\mathrm{e^+e^-} \to \tilde{\ell}_{\mathrm{R}}\bar{\tilde{\ell}}_{\mathrm{R}}$ for $\mu = -200$ GeV and $\tan\beta = 2$. These exclusions hold for $\tan\beta \geqslant 2$ and $|\mu| \geqslant 200$.

Under these assumptions, 95% CL lower limits on the masses of scalar leptons are derived as 94.4 GeV for scalar electrons with $\Delta M > 10$, 86.7 GeV for scalar muons with $\Delta M > 10$ and 78.3 GeV for scalar taus with $\Delta M > 15$ GeV.

The limiting factor towards an absolute limit on the scalar electron mass is the lack of detection efficiency for very small ΔM values. This is overcome, in the constrained MSSM, by using the $\mathrm{e^+e^-} \to \tilde{\mathrm{e}}_{\mathrm{R}}\tilde{\mathrm{e}}_{\mathrm{L}}$ process. The searches for acoplanar electrons and single electrons are combined to derive a lower limit on $M_{\tilde{\mathrm{e}}_{\mathrm{R}}}$ as a function of $\tan\beta$ and for any value of m_0, M_2 and μ as shown in Fig. 5(a). For $\tan\beta < 1$ the mass difference between $\tilde{\mathrm{e}}_{\mathrm{L}}$ and $\tilde{\mathrm{e}}_{\mathrm{R}}$ decreases, reducing the sensitivity of the single electron search. As an example, Fig. 5(b) shows the limit as a function of m_0 for a fixed value of $\tan\beta$. For $\tan\beta \geqslant 1$, the 95% CL lower limit for the lightest scalar electron, independent of the MSSM parameters, is

$$M_{\tilde{\mathrm{e}}_{\mathrm{R}}} \geqslant 71.3\ \text{GeV}.$$

Assuming a common mass for the scalar leptons at the GUT scale, this limit holds for the lightest scalar muon, $\tilde{\mu}_{\mathrm{R}}$, as well.

5.2. Limits on scalar quark masses

Fig. 6(a) shows the excluded $\tilde{\mathrm{t}}_1$ mass region as a function of $M_{\tilde{\mathrm{t}}_1}$ and $M_{\tilde{\chi}_1^0}$ at $\cos\theta_{\mathrm{LR}} = 1$ and $\cos\theta_{\mathrm{LR}} = 0.57$ for the $\tilde{\mathrm{t}}_1 \to \mathrm{c}\tilde{\chi}_1^0$ decay. The second value of the mixing angle corresponds to a vanishing contribution of the Z exchange in the s-channel production. For

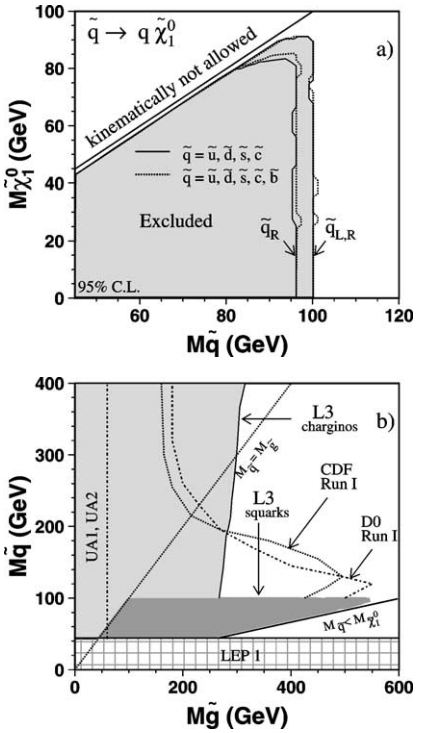

Fig. 7. (a) MSSM exclusion limits in the $M_{\tilde{\chi}_1^0}$–$M_{\tilde{q}}$ plane for degenerate scalar quarks decaying via $\tilde{q} \to q\tilde{\chi}_1^0$. (b) Excluded regions in the $M_{\tilde{g}}$–$M_{\tilde{q}}$ plane. The dark shaded area is excluded by the search for scalar quarks of the first two families, assuming mass degeneracy among different flavours and between left- and right-handed scalar quarks. The light shaded area illustrates indirect limits on the gluino mass, derived from the chargino, neutralino and scalar lepton searches. The regions excluded by the CDF and D0 Collaborations [8] are valid for $\tan\beta = 4$ and $\mu = -400$ GeV. The exclusions obtained by the UA1 and UA2 Collaborations [28] are also shown.

this decay mode, scalar top masses below 95 GeV are excluded at 95% CL under the assumptions $\cos\theta_{\mathrm{LR}} = 1$ and $\Delta M = 15$–25 GeV. For the same values of ΔM and in the most pessimistic scenario of $\cos\theta_{\mathrm{LR}} = 0.57$, the 95% CL mass limit is 90 GeV. The region in which the $\tilde{t}_1 \to bW\tilde{\chi}_1^0$ decay is kinematically accessible and becomes the dominant decay mode, is indicated. This decay is not considered in this analysis.

Fig. 6(b) shows the scalar top mass regions which are excluded if the dominant three-body decay $\tilde{t}_1 \to b\ell\tilde{\nu}$ is kinematically accessible. Equal branching fractions for the decays into e, μ or τ are assumed and 95% CL mass lower limits are derived as 96 and 93 GeV for $\cos\theta_{\mathrm{LR}} = 1$ and $\cos\theta_{\mathrm{LR}} = 0.57$, respectively. The corresponding exclusion limits for the scalar top decay $\tilde{t}_1 \to b\tau\tilde{\nu}$ are shown in Fig. 6(c). Mass lower limits at 95% CL in the range 93–95 GeV are obtained, assuming $\Delta M > 15$ GeV.

Fig. 6(d) shows the region excluded as a function of $M_{\tilde{b}_1}$ and $M_{\tilde{\chi}_1^0}$ considering the $\tilde{b}_1 \to b\tilde{\chi}_1^0$ decay for $\cos\theta_{\mathrm{LR}} = 1$ and $\cos\theta_{\mathrm{LR}} = 0.39$. The latter value corresponds to a vanishing contribution of the Z exchange in the s-channel production. Scalar bottom masses below 95 GeV are excluded at 95% CL assuming $\cos\theta_{\mathrm{LR}} = 1$ and $\Delta M = 15$–25 GeV. For $\cos\theta_{\mathrm{LR}} = 0.39$, the 95% CL mass lower limit is 81 GeV.

For scalar quarks of the first two generations, the same selection efficiencies are assumed as for the $\tilde{t}_1 \to c\tilde{\chi}_1^0$ decay because of the similar event topologies. The cross section limits given in Fig. 3(a) are then interpreted in terms of degenerate scalar quark masses. Fig. 7(a) shows the scalar quark mass lower limits as a function of the $\tilde{\chi}_1^0$ mass. Two scenarios are considered: left- and right-handed scalar quark degeneracy or only right-handed scalar quark production. In the first case, with four degenerate scalar quark flavours, the 95% CL mass limit is 99.5 GeV at for $\Delta M > 10$ GeV. In the case of only right-handed scalar quark production, the 95% CL mass lower limit is 97 GeV. Regions excluded in the hypotheses that all scalar quarks but the scalar top are degenerate are also shown.

Assuming gaugino unification at the GUT scale, the results for the four degenerate scalar quarks are reinterpreted on the plane of the scalar quark and gluino masses, as shown in Fig. 7(b). In addition, gaugino unification [25] allows a transformation of the absolute limit on M_2, obtained from the chargino and neutralino [26] as well as scalar lepton searches, into a lower limit on the gluino mass, also shown in Fig. 7(b). The ISAJET program [27] is used for the calculation of the exclusion contours. For $\tan\beta = 4$, gluino masses up to about 270–310 GeV are excluded at 95% CL.

In conclusion, no evidence for the production of scalar lepton and quarks is observed in the data set collected by the L3 experiment at LEP. Stringent upper limits on the cross sections for the production of these scalar particles are derived, which correspond to lower mass limits in the MSSM.

References

[1] Yu.A. Golfand, E.P. Likhtman, Sov. Phys. JETP 13 (1971) 323;
D.V. Volkhov, V.P. Akulov, Phys. Lett. B 46 (1973) 109;
J. Wess, B. Zumino, Nucl. Phys. B 70 (1974) 39;
P. Fayet, S. Ferrara, Phys. Rep. C 32 (1977) 249;
A. Salam, J. Strathdee, Fortschr. Phys. 26 (1978) 57.

[2] H.P. Nilles, Phys. Rep. 110 (1984) 1;
H.E. Haber, G.L. Kane, Phys. Rep. 117 (1985) 75;
R. Barbieri, Nuovo Cimento 11 (4) (1988) 1.

[3] C. Bohem, A. Djouadi, Y. Mambrini, Phys. Rev. D 61 (2000) 0950006, and references therein.

[4] L3 Collaboration, P. Achard, et al., Phys. Lett. B 524 (2002) 65.

[5] L3 Collaboration, M. Acciarri, et al., Phys. Lett. B 471 (1999) 280, and references therein.

[6] L3 Collaboration, M. Acciarri, et al., Phys. Lett. B 471 (1999) 308, and references therein.

[7] ALEPH Collaboration, R. Barate, et al., Phys. Lett. B 537 (2002) 5;
ALEPH Collaboration, R. Barate, et al., Phys. Lett. B 526 (2002) 206;
ALEPH Collaboration, R. Barate, et al., Phys. Lett. B 544 (2002) 73;
DELPHI Collaboration, P. Abreu, et al., Eur. Phys. J. C 13 (2000) 29;
DELPHI Collaboration, P. Abreu, et al., Phys. Lett. B 496 (2000) 59;
OPAL Collaboration, G. Abbiendi, et al., Phys. Lett. B 545 (2002) 272;
OPAL Collaboration, G. Abbiendi, et al., Eur. Phys. J. C 14 (2000) 51.

[8] CDF Collaboration, F. Abe, et al., Phys. Rev. D 56 (1997) 1357;
D0 Collaboration, S. Abachi, et al., Phys. Rev. Lett. 75 (1995) 618.

[9] L3 Collaboration, B. Adeva, et al., Nucl. Instrum. Methods A 289 (1990) 35;
M. Chemarin, et al., Nucl. Instrum. Methods A 349 (1994) 345;
M. Acciarri, et al., Nucl. Instrum. Methods A 351 (1994) 300;
G. Basti, et al., Nucl. Instrum. Methods A 374 (1996) 293;
I.C. Brock, et al., Nucl. Instrum. Methods A 381 (1996) 236;
A. Adam, et al., Nucl. Instrum. Methods A 383 (1996) 342.

[10] PYTHIA version 5.722 is used:
T. Sjöstrand, preprint CERN-TH/7112/93, revised August 1995;
T. Sjöstrand, Comput. Phys. Commun. 82 (1994) 74;
T. Sjöstrand, hep-ph/0001032.

[11] EXCALIBUR Monte Carlo: F.A. Berends, R. Kleiss, R. Pittau, Comput. Phys. Commun. 85 (1995) 437.

[12] KORALZ version 4.02 is used: S. Jadach, B.F.L. Ward, Z. Wąs, Comput. Phys. Commun. 79 (1994) 503.

[13] BHWIDE version 1.01 is used: S. Jadach, W. Placzek, B.F.L. Ward, Phys. Lett. B 390 (1997) 298.

[14] KORALW version 1.33 is used:
S. Jadach, et al., Comput. Phys. Commun. 94 (1996) 216;
S. Jadach, et al., Phys. Lett. B 372 (1996) 289.

[15] DIAG36 Monte Carlo: F.A. Berends, P.H. Daverveldt, R. Kleiss, Nucl. Phys. B 253 (1985) 441.

[16] PHOJET version 1.05 is used:
R. Engel, Z. Phys. C 66 (1995) 203;
R. Engel, J. Ranft, Phys. Rev. D 54 (1996) 4244.

[17] SUSYGEN Monte Carlo: S. Katsanevas, et al., Comput. Phys. Commun. 112 (1998) 227.

[18] Modified version of the OPAL MC generator for scalar quarks production: E. Accomando, et al., in: G. Altarelli, T. Sjöstrand, F. Zwirner (Eds.), Physics at LEP2, vol. 2, CERN, Geneva, 1996, p. 343, CERN 96-01.

[19] K. Hagiwara, et al., Phys. Rev. D 66 (2002) 010001.

[20] GEANT version 3.15 is used: R. Brun, et al., preprint CERN DD/EE/84-1, revised 1987.

[21] H. Fesefeldt, RWTH Aachen Report PITHA 85/2, 1985.

[22] L3 Collaboration, M. Acciarri, et al., Eur. Phys. J. C 4 (1998) 207.

[23] S. Bethke, et al., Nucl. Phys. B 370 (1992) 310, and references therein.

[24] R.D. Cousins, V.L. Highland, Nucl. Instrum. Methods A 320 (1992) 331.

[25] L.E. Ibanez, Phys. Lett. B 118 (1982) 73;
R. Barbieri, S. Ferrara, C. Savoy, Phys. Lett. B 119 (1982) 343.

[26] L3 Collaboration, M. Acciarri, et al., Search for charginos and neutralinos in e^+e^- collisions up to $\sqrt{s} = 209$ GeV, in preparation.

[27] H. Baer, et al., in: J. Hewett, D. Zeppenfeld (Eds.), Proceedings of the Workshop on Physics at Current Accelerators and Supercolliders, Argonne National Laboratory, Argonne, IL, 1993.

[28] UA1 Collaboration, C. Albajar, et al., Phys. Lett. B 198 (1987) 261;
UA2 Collaboration, J. Alitti, et al., Phys. Lett. B 235 (1990) 363.